# Functional $GABA_A$ Receptor Heterogeneity of Acutely Dissociated Hippocampal CA1 Pyramidal Cells

ELIZABETH I. TIETZ,[1] JAIDEEP KAPUR,[2] AND ROBERT L. MACDONALD[2,3]
[1]*Department of Pharmacology, Medical College of Ohio, Toledo, Ohio 43614-5804; and Departments of* [2]*Neurology and* [3]*Physiology, University of Michigan, Ann Arbor, Michigan 48104-1687*

**Tietz, Elizabeth I., Jaideep Kapur, and Robert L. Macdonald.** Functional $GABA_A$ receptor heterogeneity of acutely dissociated hippocampal CA1 pyramidal cells. *J. Neurophysiol.* 81: 1575–1586, 1999. CA1 pyramidal cells were voltage clamped, and GABA was applied to individual cells with a modified U-tube, rapid drug application system. With $V_h$ = −50 mV, inward currents elicited by 10 $\mu$M GABA were inhibited by $GABA_A$ receptor (GABAR) antagonists and were baclofen insensitive, suggesting that GABA actions on isolated CA1 pyramidal cells were GABAR mediated. GABA concentration-response curves averaged from all cells were fitted best with a two-site equation, indicating the presence of at least two GABA binding sites, a higher-affinity site ($EC_{50-1}$ = 11.0 $\mu$M) and a lower-affinity site ($EC_{50-2}$ = 334.2 $\mu$M), on two or more populations of cells. The effects of GABAR allosteric modulators on peak concentration-dependent GABAR currents were complex and included monophasic (loreclezole) or multiphasic (diazepam) enhancement, mixed enhancement/inhibition (DMCM, zolpidem) or multiphasic inhibition (zinc). Monophasic (70% of cells) or biphasic (30% of cells) enhancement of GABAR currents by diazepam suggested three different sites on GABARs ($EC_{50-1}$ =1.8 nM; $EC_{50-2}$ = 75.8 nM; $EC_{50-3}$ = 275.9 nM) revealing GABAR heterogeneity. The imidazopyridine zolpidem enhanced GABAR currents in 70% of cells with an $EC_{50}$ = 222.5 nM, suggesting a predominance of moderate affinity $\alpha$2 (or $\alpha$3-) subtype-containing BZ Type IIA receptors. A small fraction of cells (10%) had a high affinity for zolpidem, something that is suggestive of $\alpha$1 subtype-containing BZ Type I receptors. The remaining 30% of cells were insensitive to or inhibited by zolpidem, suggesting the presence of $\alpha$5 subtype-containing BZ Type IIB receptors. Whether BZ Type I and Type II receptors coexist could not be determined. The $\beta$-carboline methyl 6,7-dimethoxy-4-ethyl-$\beta$-carboline-3-carboxylate (DMCM) inhibited GABAR currents in all cells at midnanomolar concentrations, but in addition, potentiated GABAR currents in some cells at low nanomolar concentrations, characterizing two groups of cells, the latter likely due to functional assembly of $\alpha$5$\beta$x$\gamma$2GABARs. In all cells, GABAR currents were moderately sensitive ($EC_{50}$ = 9 $\mu$M) to loreclezole, consistent with a relatively greater $\beta$3 subtype, than $\beta$1 subtype, subunit mRNA expression. Two populations of cells were identified based on their sensitivities to zinc($IC_{50}$ = 28 and 182 $\mu$M), suggesting the presence of at least two GABAR isoforms including $\alpha$5$\beta$3$\gamma$2 GABARs. Consistent with the heterogeneity of expression of GABAR subunit mRNA and protein in the hippocampus and based on their differential responses to GABA and to allosteric modulators, distinct populations of CA1 pyramidal cells likely express multiple, functional GABAR isoforms.

## INTRODUCTION

$\gamma$-Aminobutyric acid (GABA) mediates fast inhibitory synaptic transmission by opening the $GABA_A$ receptor (GABAR) chloride ion channel, a hetero-oligomeric pentamer (Nayeem et al. 1994). GABAR currents are enhanced by several clinically useful drugs, including barbiturates, benzodiazepines, and imidazopyridines that act at different allosteric regulatory sites on GABARs. Additional modulatory sites have been described for negative modulators of GABARs such as the $\beta$-carbolines and zinc (Macdonald and Olsen 1994; Smart et al. 1991). Heterogeneity of native GABARs was suggested by classical pharmacological studies of allosteric modulators that identified receptors with different drug sensitivities (BZ Type I and II) (Burt and Kamatchi 1991; Ehlert et al. 1983). Heterogeneity of GABARs was supported by the identification of different GABAR subunit families with multiple subtypes [$\alpha$(1–6), $\beta$(1–4), $\gamma$(1–4), $\delta$(1), and $\epsilon$(1)] displaying different pharmacological properties in recombinant expression systems (Davies et al. 1997; Macdonald and Angelotti 1993; Macdonald and Olsen 1994; Vincini 1991).

Studies in heterologous expression systems have shown that distinct pharmacological properties are conferred by varying GABAR subunit composition. For example, the $\alpha$ subtype is a primary determinant of benzodiazepine and imidazopyridine sensitivity [$\alpha$1 (Type I); $\alpha$2 and $\alpha$3 (Type IIA); $\alpha$5 (Type IIB) and $\alpha$4 and $\alpha$6 (Type III)] (Doble and Martin 1992; Pritchett et al. 1989; Wieland et al. 1992). Loreclezole, a novel antiepileptic drug, enhances currents from GABARs assembled with $\beta$2 and $\beta$3 subtypes but not with the $\beta$1 subtype (Wafford et al. 1994). A $\gamma$ subunit is required to achieve the full range of benzodiazepine effects (Pritchett et al. 1989) and also results in relative zinc insensitivity (Draguhn et al. 1990; Smart et al. 1991), depending on the $\alpha$ subtype present (Saxena and Macdonald 1996). GABARs containing $\alpha$4 or $\alpha$6 subunits are benzodiazepine insensitive and have relatively high zinc sensitivity (Davies et al. 1997; Saxena and Macdonald 1994, 1996). Thus GABAR pharmacological properties are determined by $\alpha$, $\beta$, and $\gamma$ subunit subtypes (Ducic et al. 1995; Ebert et al. 1994; Hadingham et al. 1993).

GABARs play a prominent role in modulation of CNS excitability (Stelzer 1992) and have a dense, heterogeneous distribution in the CA1 region of the hippocampus (Olsen et al. 1990). In situ hybridization studies of the CA1 region of the hippocampus have demonstrated that $\alpha$2, $\alpha$5, $\beta$1, $\beta$3, and $\gamma$2 subtype mRNAs are highly expressed, $\alpha$1 and $\alpha$4 subtype mRNAs are moderately expressed, $\alpha$3, $\beta$2, and $\gamma$1 subtype mRNAs are minimally expressed, and $\alpha$6, $\gamma$3, and $\delta$1 subtype mRNAs are negligibly expressed or are absent (Wisden et al. 1992). The relative expression of GABAR subunit mRNAs may reflect their subunit protein expression on CA1 pyramidal

The costs of publication of this article were defrayed in part by the payment of page charges. The article must therefore be hereby marked ''*advertisement*'' in accordance with 18 U.S.C. Section 1734 solely to indicate this fact.

cells, and certain immunohistochemically identified GABAR subunits exist only at subsets of synapses on CA1 pyramidal cell somata and dendrites (Fritschy and Möhler 1995; Nusser et al. 1996; Somogyi et al. 1996; Sperk et al. 1997; E. I. Tietz, S. Chen, and W. Sieghart, unpublished observations). The diversity of subtype mRNA and protein expression and the compartmentalization of subunit subtypes suggest that multiple GABAR isoforms may be assembled on individual CA1 pyramidal cells to produce functionally distinct GABARs. The heterogeneity of CA1 pyramidal cell GABARs was deduced from early pharmacological studies in in vitro hippocampus (Alger and Nicoll 1982). Functional heterogeneity of GABARs was later reported in hippocampal CA1 cells in culture (Schönrock and Bormann 1993) and more recently physiologically distinct GABAR currents, which may arise from different classes of GABAergic interneurons (Freund and Buszáki 1996; Lacaille et al. 1989; Miles et al. 1996; Nusser et al. 1996), were shown to be anatomically segregated on CA1 pyramidal cell somata and dendrites (Banks et al. 1998; Pearce 1993).

The goal of the present study was to characterize the sensitivity of individual CA1 pyramidal cells to GABA and allosteric modulators and to compare the functional properties of GABARs to their proposed subunit composition. The concentration-dependent effects of various allosteric modulators that have subunit subtype-dependent actions (diazepam, zolpidem, loreclezole, DMCM, and zinc) on GABAR currents were studied in mature, acutely dissociated cells using the whole cell patch-clamp technique.

Portions of this work have appeared in *Soc. Neurosci. Abstr.* 21: 1346, 1995.

## METHODS

### *Isolation of CA1 pyramidal cells*

CA1 pyramidal cells were dissociated acutely from 28- to 35-day-old Sprague-Dawley rats (Harlan, Indianapolis, IN) using modifications of the original procedures of Kay and Wong (1986) and others (Celentano and Wong 1994; Kapur and Macdonald 1996; Oh et al. 1995). Rats were euthanized with $CO_2$ and decapitated, and the brain was rapidly dissected free. The region containing the hippocampus was blocked and placed for 1 min in ice-cold (4°C), oxygenated (95% $O_2$-5% $CO_2$) 1,4-piperazinebis(ethanesulfonic acid (PIPES) buffer containing (in mM) 120 NaCl, 2.5 KCl, 1 $MgCl_2$, 1.5 $CaCl_2$, 25 D-glucose, and 20 PIPES, pH 7.0. Coronal slices (500 $\mu$m) were cut on a vibroslice (Campden Instruments, Campden, U.K.) in preoxygenated, PIPES buffer maintained at 4°C, then were incubated for a minimum of 1 h at room temperature (24°C) in continuously oxygenated PIPES buffer. One or two slices were incubated in Type XXIII protease (3 mg/ml, Sigma Chemical, St. Louis, MO) in oxygenated PIPES buffer for 30 min at 32°C. After an additional 15–60 min recovery in PIPES buffer at room temperature, cells were isolated acutely by trituration of two to three 1-mm fragments microdissected from the CA1 region of the right or left hippocampus. Cells were plated in extracellular recording buffer (see next section) on poly-L-lysine-coated (0.1 mg/ml in 0.1 M boric acid/0.1 M Na tetraborate, pH 8.4) 35-mm culture dishes, were allowed to adhere to the plate for ≥10 min, and were used for electrophysiological recording within 1 h of dissociation.

### *Electrophysiological recording*

Whole cell voltage-clamp recordings ($V_h = -50$ mV) were made from isolated pyramidal cells according to Hamill et al. (1981). The bathing solution contained (in mM) 142 NaCl, 1 $CaCl_2$, 8.1 KCl, 6 $MgCl_2$, 10 D-glucose, and 10 HEPES (Burgard et al. 1996; Saxena and Macdonald 1996). The pH was adjusted to 7.4 with 5 M NaOH, and the osmolarity to 322–326 mOsm. Patch pipettes were thin-wall, filamented borosilicate glass capillaries (1.5 mm OD, World Precision Instruments, Sarasota, FL) pulled to a tip resistance of 6–10 MΩ on a Flaming-Brown electrode puller (P-87, Sutter Instruments, San Rafael, CA) using a two-stage pull. To facilitate gigaohm seal formation, the patch pipettes were front-filled (500 $\mu$m) with internal solution [which contained (in mM) 155.3 KCl, 1 $MgCl_2$, 10 HEPES, and 5 EGTA, pH 7.3] adjusted to 285–287 mOsm. The shank was back-filled with the same internal solution containing an ATP regeneration system (50 U/ml creatinine phosphokinase, 22 mM phosphocreatine, and 4 mM MgATP, 297–299 mOsm).

Currents were recorded at room temperature using a List EPC-7 patch-clamp amplifier (List Electronics, Eberstadt, Germany) and low-pass filtered at 2 kHz with an eight-pole Bessel filter (Frequency Devices, Haverhill, MA). Whole cell currents were displayed on a Gould 2400S chart recorder and recorded for later analysis onto computer hard disk using a TL-1 AD/DA converter and Axotape 2.0 acquisition and analysis software (Axon Instruments, Foster City, CA). Peak current responses were measured off-line from the digitized current traces using Axotape 2.0 analysis software. Peak current (pA) was defined as the initial maximal negative deflection from the baseline value determined immediately before the onset of the drug response.

### *Drug solutions and drug application*

Drug application was gravity driven through a glass micropipette tip (30- to 50-$\mu$m tip diameter) positioned within 50–100 $\mu$m of an individual pyramidal cell. All drug solutions were applied to individual cells at 1-min intervals using this modified U-tube ''multipuffer'' drug-application system (Greenfield and Macdonald 1996). A constant negative pressure prevented the flow of buffer (or drug) from the tip of the drug-application micropipette. The length of the drug-application bar (Figs. 2–8) represented the total activation time (5–12 s) of a normally ''open'' solenoid valve. The solenoid, when closed, interrupted the negative pressure, allowing solution to flow. The response time of the solenoid valve was 8–15 ms. An additional ''lag time'' was introduced between solenoid closure and drug application, before the onset of the GABA-mediated current response, due to the small amount of buffer that flowed through the coupled micropipette before test drug flow. The duration of solenoid activation was varied as a function of the exact placement of the multipuffer relative to the recorded cell. The response characteristics of the ''multipuffer'' were determined previously by measuring the change in tip potential of an open electrode to step changes of $K^+$ ($\tau = 23.0$ ms; total solution exchange time 101.4 ms) (Greenfield and Macdonald 1996). Before each recording session, the area of drug application was visualized with Fast Green and included the entire area occupied by individual cells. Solutions were dissolved in extracellular buffer to the desired concentrations from the following stock solutions: 100 mM GABA in $H_20$; 10 mM bicuculline methobromide in $H_2O$; 20 mM picrotoxin in 100% EtOH; 10 mM diazepam in DMSO; 0.4 mM zolpidem in $H_2O$; 100 mM loreclezole in DMSO; 10 mM DMCM in DMSO; and 100 mM $ZnCl_2$ in $H_2O$. Drugs dissolved in DMSO or ethanol were diluted further in extracellular buffer to a final concentration of <0.05%. The vehicles alone or when coapplied with 5 or 10 $\mu$M GABA had no effect on CA1 pyramidal cell GABAR whole cell currents. Coapplied drug solutions were maintained in the same drug reservoir. GABA, bicuculline methobromide, picrotoxin, and $ZnCl_2$ and all other chemicals were purchased from Sigma Chemical. Diazepam was a gift from Hoffmann La-Roche Incorporated (Nutley, NJ). Zolpidem was from Research Biochemicals International (Natick, MA). Loreclezole was a gift from Janssen Pharmaceutical (Belgium).

### *GABA and allosteric modulator effects on CA1 pyramidal cells*

To evaluate GABA concentration-response relationships in CA1 pyramidal cells, the maximal currents induced at each of five to eight GABA concentrations were compared in the 19 cells tested. To evaluate allosteric modulator effects on CA1 pyramidal cell GABA-induced currents, diazepam, zolpidem, loreclezole, DMCM, and zinc were coapplied with 10 $\mu$M GABA. Because loreclezole only minimally enhanced currents induced by 10 $\mu$M GABA, loreclezole also was coapplied with 5 $\mu$M GABA. The concentration of GABA was chosen to be on the linear portion of the GABA concentration-response curve, thus allowing a reliable measure of both the potentiation and inhibition produced by the various modulators. The effect of GABA-induced current desensitization on the assessment of peak current also was minimized at lower GABA concentrations (Celentano et al. 1991).

### *Data analysis*

Peak GABAR current amplitudes were analyzed for each cell as described above. To evaluate the CA1 pyramidal cell population responses, individual peak current amplitudes were normalized, i.e., defined as 100% for each cell. Individual and averaged GABA concentration-response data were fit to a one-site model by nonlinear regression with the equation

$$I = [I_{(\min)} + I_{(\max)}([\mathrm{GABA}]^n/\mathrm{EC}_{50}^n)]/(1 + [\mathrm{GABA}]^n/\mathrm{EC}_{50}^n) \quad (1)$$

or a two-site model with the equation

$$I = [I_{(\min 1)} + I_{(\max 1)}([\mathrm{GABA}]^n/\mathrm{EC}_{50\text{-}1}^n)]/(1 + [\mathrm{GABA}]^n/\mathrm{EC}_{50\text{-}1}^n) + [I_{(\min 2)} + I_{(\max 2)}([\mathrm{GABA}]^n/\mathrm{EC}_{50\text{-}2}^n)]/(1 + [\mathrm{GABA}]^n/\mathrm{EC}_{50\text{-}2}^n) \quad (2)$$

where $I$ was the current at a given GABA concentration, $I_{(\min)}$ was the current in the absence of GABA, and $I_{(\max)}$ was the current evoked by a saturating GABA concentration. The Hill slope ($n_H$) was allowed to vary. For each cell tested and for the averaged data, a comparison of the goodness-of-fit of the data points to a one- or a two-site model was made by $F$ test. The equation for the $F$ ratio [(SS1-SS2)/(df1-df2]/[SS2/df2] was derived from the sum of squares (SS) of the residuals from each curve and the respective degrees of freedom (df), i.e., the number of data points minus the number of variables. A two-site model was considered to fit the data points significantly better than a one-site fit if $P < 0.05$. The $EC_{50}$s were derived from the best-fit equation.

The concentration-response relationships for allosteric modulators were constructed by evaluating the degree of potentiation or inhibition achieved by coapplication of each allosteric modulator and were expressed as a fraction of the control GABAR whole cell current. The peak amplitudes of the GABAR currents in the presence of various concentrations of each allosteric modulator were taken as fractions of the average responses to GABA applied 1 min before and 1 min after coapplication of each concentration. The fractions of the average GABA-response were multiplied by 100 and expressed as percent control, i.e., the control GABA-responses were set equal to 100%.

For diazepam and zolpidem, which also binds to the benzodiazepine binding site, a comparison of the peak current amplitudes obtained with each allosteric-modulator concentration were compared with an equation for a one-site model

$$I/I_{\mathrm{dmin}} = [1 + I_{\mathrm{dmax}}/I_{\mathrm{dmin}}*([\mathrm{Drug}]/\mathrm{EC}_{50})]/(1 + [\mathrm{Drug}]/\mathrm{EC}_{50}) \quad (3)$$

or a two-site model

$$I/I_{\mathrm{dmin}} = [1 + I_{\mathrm{dmax1}}/I_{\mathrm{dmin}}*([\mathrm{Drug}]/\mathrm{EC}_{50\text{-}1})]/(1 + [\mathrm{Drug}]/\mathrm{EC}_{50\text{-}1}) + [1 + I_{\mathrm{dmax2}}/I_{\mathrm{dmin}}*([\mathrm{Drug}]/\mathrm{EC}_{50\text{-}2})]/(1 + [\mathrm{Drug}]/\mathrm{EC}_{50\text{-}2}) \quad (4)$$

where $I_{\mathrm{dmin}}$ was the current in the absence of drug and $I_{\mathrm{dmax}}$ was the current as allosteric modulator concentration approached infinity. Concentration-response curves for diazepam also were fit with the one- or two-site equations described by Oh et al. (1995) where $n_H$ was allowed to vary or was set = 2. Based on the $EC_{50}$s obtained from individual fits (Fig. 4*D*, *inset*), the averaged responses of cells tested with diazepam were fit to a one-, two-, or three-site model with $n_H = 1$. Best-fit comparisons between one- and two-site or two- and three-site fits were made by $F$ test ($P < 0.05$) as described in the preceding text.

No a priori assumptions were made with regard to the mechanism of action of loreclezole and zinc at the GABAR, and their effects on GABAR currents were compared with a four-parameter logistic equation

$$I = I_{\min} + (I_{\max} - I_{\min})/(1 + 10^{(\log \mathrm{EC50\text{-}[Drug]})*n_H}) \quad (5)$$

in which $n_H$ was allowed to vary. Although DMCM is known to interact directly or allosterically with the benzodiazepine receptor, the variable DMCM concentration-response curves also were fit with *Eq. 5* for a sigmoidal dose-response curve. All curve fits and comparisons of goodness-of-fit were carried out using PRISM software (GraphPAD, San Diego, CA).

## RESULTS

### *Acutely dissociated CA1 pyramidal cell morphology*

Because response heterogeneity may depends on the cell preparation, it was important to specify the cells used in the study. In each dish 5–20 CA1 pyramidal cells were suitable for whole cell recording based on their phase-bright appearance and distinct morphological characteristics (Fig. 1). Cells selected had a diameter >20 $\mu$m and were pyramidal or polygonal in shape. The cells had a single large principle dendrite of ≥60–80 $\mu$m in length, although a majority of cells selected had apical dendrites >120–150 $\mu$m long. Longer dendrites, i.e., 200 $\mu$m, occasionally were branched. Fusiform cells with an ovoid appearance, multipolar cells with diffuse processes, and small granule cells from the overlying dentate gyrus occasionally were present and were rejected for study.

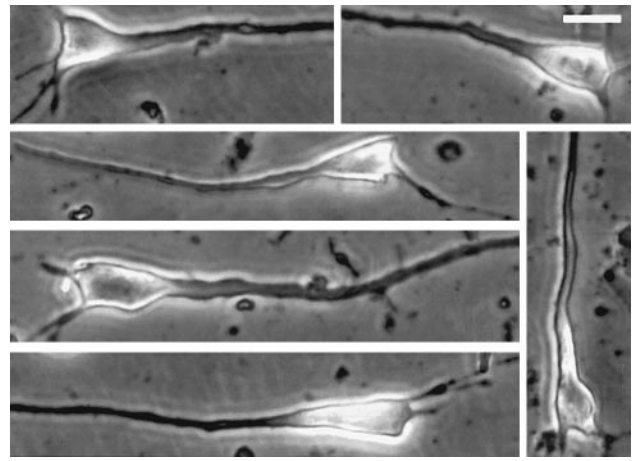

FIG. 1. Characteristics of acutely dissociated CA1 pyramidal cells. Phase contrast photomicrographs of typical CA1 pyramidal cells isolated from a 30-day-old rat. Acutely dissociated cells retained their somata and proximal dendrites. One to 3 basal dendrites 20–30 $\mu$m in length and the axon hillock usually were preserved. Apical dendrites ranged from 20–200 $\mu$m (median 100–120 $\mu$m) in length and were occasionally branched. Scale bar = 20 $\mu$m.

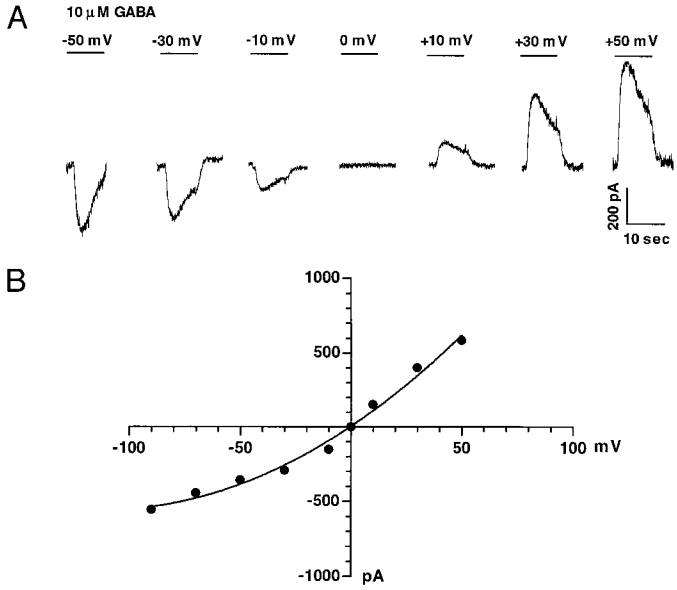


FIG. 2. $GABA_A$ receptor (GABAR) current-voltage relationship in CA1 pyramidal cells. *A*: response to 10 $\mu$M GABA of a CA1 pyramidal cell voltage clamped to the potentials indicated *above* each trace. Horizontal bars indicate the duration of activation of the solenoid that delivered GABA to the multipuffer tip. The onset of the GABAR current occurred with a delay because the line connected to the multipuffer contained control solution that was ejected before the ejection of GABA. *B*: peak current-voltage relationship was determined for a range of holding potentials ($V_h$ = −90 to +50 mV). With nearly symmetrical [$Cl^-$] inside and outside the pyramidal cell, $E_{GABA}$ was near 0 mV (−1.6 ± 1.7 mV, $n$ = 4). Note the outward rectification of the current response.

### *CA1 pyramidal cell currents*

Whole cell recordings were made in nearly symmetrical chloride ion solutions ($[Cl^-]_o$ = 164 mM; $[Cl^-]_i$ = 155 mM; $E_{Cl^-}$ = 1.4 mV). GABA evoked inward currents at negative membrane holding potentials and outward currents at positive holding potentials (Fig. 2*A*). The GABAR current reversal potential ($E_{GABA}$) was −1.6 ± 1.7 (SE) mV ($n$ = 4 cells) equivalent to the $E_{Cl^-}$ predicted by the Nernst equation. A plot of the peak *I-V* relationship generated in an individual CA1 pyramidal cell for $V_h$s ranging from −90 to +50 mV is shown in Fig. 2*B*.

Without ATP in the recording pipette, repetitive application of GABA produced currents that declined in amplitude with each successive GABA application (current rundown). To minimize current rundown, ATP and an ATP regeneration system were included in the intrapipette recording solution (Oh et al. 1995; Stelzer et al. 1988). Stable recordings could be maintained for ≤1 h, although a slow rundown or run-up occasionally was detected. Therefore to control for any small degree of rundown that may have occurred despite inclusion of an ATP regeneration system in the patch pipette, the effects of varying concentrations of allosteric modulators were assessed as a fraction of the averaged baseline GABAR current before and after test drug applications. Cells with current rundown of >80% over the lifetime of the recording were not included in the analysis. Although multiple test drugs occasionally were applied to the same cells, it was generally not possible to obtain full concentration-response curves for more than a single drug to make reliable cross-drug comparisons of $EC_{50}$s.

Unless otherwise noted, inward currents were elicited from pyramidal cells by 10 $\mu$M GABA at $V_h$ = −50 mV. The competitive antagonist bicuculline methobromide (10 and 50 $\mu$M) completely and reversibly inhibited the GABAR currents (data not shown). After GABAR activation, the noncompetitive antagonist picrotoxin (100 $\mu$M) also inhibited GABAR currents (data not shown). The inhibition by picrotoxin reversed slowly (>5 min). The $GABA_B$ agonist baclofen (0.1 and 1.0 $\mu$M; $V_h$ = −50 to +30 mV) was applied to pyramidal cells 5 min after current activation by 10 $\mu$M GABA. Baclofen failed to evoke currents in four of four cells (data not shown). Taken together, these results suggested that GABA currents elicited from CA1 pyramidal cells were mediated by GABARs.

### *Heterogeneous GABA concentration response in CA1 pyramidal cells*

Peak current amplitude increased with increasing GABA concentration (Fig. 3, *A* and *B*). Maximal current amplitude in single neurons ranged from 120 to 2,056 pA. For each cell, the one- or two-site best fit to the GABA concentration-response curves were statistically compared ($P < 0.05$). GABAR currents were monophasic in 8 of 19 cells and biphasic in 11 of 19 cells tested. There were no apparent morphological differences between CA1 pyramidal cells with monophasic or biphasic GABA concentration-response curves. Current traces for cells representative of each type are shown in Fig. 3, *A* and *B*. Examples of the best fit to GABA concentration-response curves derived from the current traces for the two cells shown in Fig. 3, *A* and *B*, displaying monophasic ($EC_{50}$ = 8.2 $\mu$M; $n_H$ = 2.9) and biphasic ($EC_{50-1}$ = 15.0 $\mu$M; $EC_{50-2}$ = 370.4 $\mu$M; $n_H$ = 2.3) concentration-response curves, are shown in Fig. 3*C*. For individual cells fit best to a single site, estimates of $EC_{50}$s ranged from 4.3 to 30.7 $\mu$M (median 11.3 $\mu$M). $EC_{50}$s estimated from the best-fit curve to the averaged normalized data from the eight cells exhibiting a monophasic response was 10.3 $\mu$M [95% confidence interval (CI) = 6.5–14.4 $\mu$M] with a Hill slope ($n_H$) of 1.6. Analysis of the GABA concentration-response curves for each cell that fit best to a two-site model indicated a similar range of $EC_{50}$ estimates for the high-affinity site ($EC_{50}$ = 6.1–15.0 $\mu$M). The $EC_{50}$ for the low-affinity site in 9 of 11 cells ranged from 108 to 908 $\mu$M. $EC_{50}$ estimates for the low-affinity site in 2 of 11 cells could not be accurately determined due to the fewer number of data points at very high GABA concentrations. GABA $EC_{50}$s for higher- and lower-affinity sites, estimated from the best-fit line to the averaged, normalized data from the 11 cells with biphasic responses, were 12.3 $\mu$M (95% CI = 7.8–16.7 $\mu$M) and 315.6 $\mu$M (95% CI = 153.4–477.9 $\mu$M), representing 42 and 54% of sites, respectively. The averaged relative amplitude curve derived from normalized peak GABAR currents elicited in all cells ($n$ = 19) is shown in Fig. 3*D*. The curve was fit best ($P < 0.05$) to high-affinity ($EC_{50-1}$ = 11.0 $\mu$M; 95% CI = 3.6–25.9 $\mu$M) and low-affinity ($EC_{50-2}$ = 346.2 $\mu$M; 95% CI = 121.6–570.8 $\mu$M; $n_H$ = 1.7) sites representing 38 and 62% of sites, respectively.

### *Diazepam enhancement of CA1 pyramidal cell GABAR currents*

The benzodiazepine agonist diazepam had variable effects on CA1 pyramidal cell GABAR currents recorded from acutely

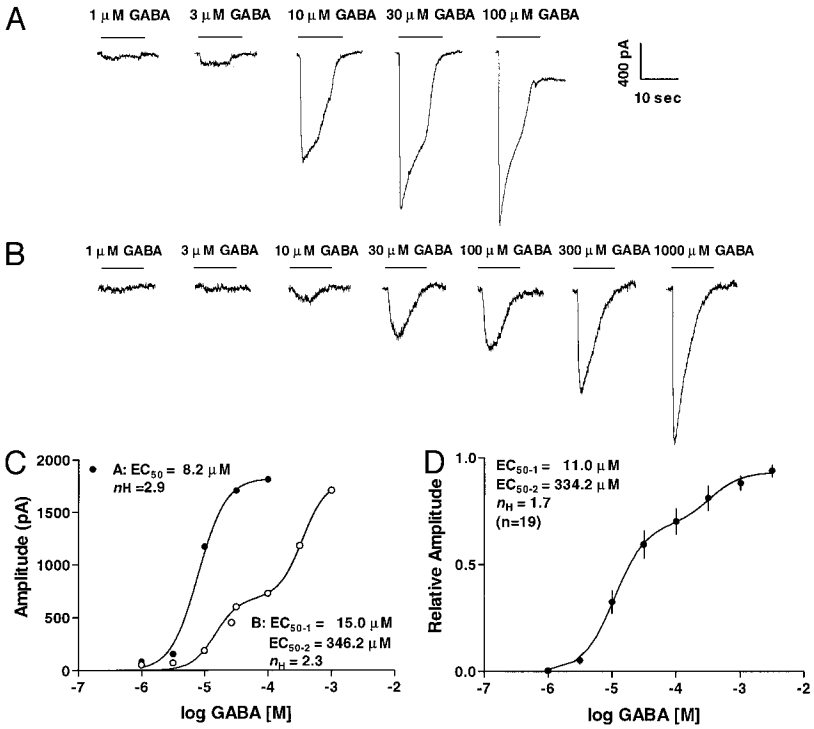


FIG. 3. GABAR whole cell currents in CA1 pyramidal cells. GABA (1–1,000 $\mu$M) was applied to single acutely dissociated CA1 pyramidal cells at 1-min intervals for the duration indicated by the horizontal bar. *A*: traces from a single cell that showed a monophasic response to GABA. Note the increased rate of activation and desensitization of the response with increasing GABA concentration. *B*: traces from a single cell that showed a biphasic response to GABA. Note the difference in the activation rate of the response in comparison to the traces in *A* indicating differences in GABA affinity in these 2 cells. *C*: concentration-response relationship for the traces in *A* and *B*. Lines represents the best fit ($P < 0.05$) of the data to 1 (*A*) or 2 sites (*B*). *D*: GABA concentration-response relationship in all CA1 pyramidal cells. Each point represents the mean ($\pm$SE) of normalized peak currents from 19 cells. Line represents the best fit ($P < 0.05$) of the data to 2 sites. $EC_{50}$s, $I_{max}$, and $n_H$ were derived from the equation for the best-fit line.

dissociated CA1 pyramidal cells. Diazepam (1–3,000 nM) was coapplied with 10 $\mu$M GABA and enhanced GABAR currents in a concentration-dependent manner (Fig. 4). GABAR current enhancement by 10 nM diazepam in individual cells varied widely. In six cells, 10 nM diazepam had little or no effect, i.e., diazepam (10 nM) enhanced the control GABAR current $<$ 10%. However, in five cells, 10 nM diazepam enhanced GABAR currents to 110–135% of control. In one cell, 10 nM diazepam enhanced GABAR currents to 160% of control. Application of 10 nM diazepam failed in one cell. A similar heterogeneous response was obtained with 100 nM diazepam. Whereas GABAR currents in all of the 13 cells were enhanced ($>$110%) by 100 nM diazepam, GABAR currents in 8 cells were potentiated to 120–135% of control. In the remaining five cells, GABAR currents were enhanced to 145–200% of control. At higher diazepam concentrations, GABAR currents were potentiated to ~130–175% (300 nM); ~150–275% (1 $\mu$M); and ~155–375% (3 $\mu$M) of control.

In 3 of the 13 cells, the concentration-response was biphasic (Fig. 4, *A* and *C*), and in the remaining 10 cells, it was monophasic (Fig. 4, *B* and *C*). $EC_{50}$s for diazepam potentiation varied widely (2.1–1167.0 nM, median 68.5 nM) as did the

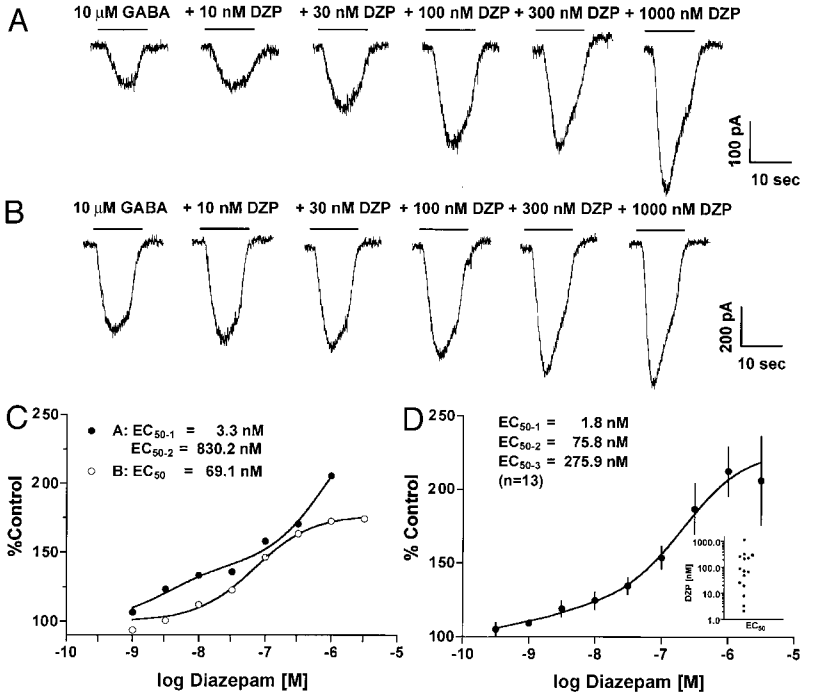


FIG. 4. Diazepam potentiation of CA1 pyramidal cell GABAR currents. Diazepam (DZP) showed multiphasic effects to enhance GABAR currents. *A*: traces from a single cell that showed a biphasic response to diazepam. Concentrations of diazepam coapplied with 10 $\mu$M GABA are indicated *above* each trace. Bars indicate the duration of solenoid activation. Not all traces are shown. *B*: traces from a different cell showing a monophasic response to diazepam coapplication. *C*: concentration-response relationship for the traces in *A* and *B*. *D*: each point represents the mean ($\pm$SE) diazepam enhancement of GABAR currents in 13 cells. Line represents the best fit of the data to 2 sites. $EC_{50}$s were derived from the equation for the best-fit line. *Inset*: $EC_{50}$s for diazepam potentiation of GABA-induced currents in the 13 cells averaged in *D* estimated from the best fits of individual concentration response curves. Additional 3 data points ($n = 16$) represent the additional $EC_{50}$ estimates in the 3 cells with a biphasic response to diazepam.

maximal enhancement achieved (155–375%, median 175). There was no correlation ($r = 0.01$) between the estimated $EC_{50}$ and the magnitude of potentiation.

Representative current traces from two cells in which diazepam was coapplied with GABA are shown in Fig. 4, *A* and *B*. The concentration-response curves derived from these individual CA1 pyramidal cell responses are shown in Fig. 4*C*. The lines represent the best fit ($P < 0.05$) of the data to one or two sites using the equations described in METHODS (Fig. 4*B*). $EC_{50}$s were derived from the equation for the best-fit lines. Diazepam had a biphasic effect ($EC_{50-1} = 2.8$ nM; $EC_{50-2} = 335.3$ nM) to enhance GABAR currents in some pyramidal cells as shown in Fig. 4*A* or a monophasic effect ($EC_{50} = 57.1$ nM, $E_{max} = 178.3 \pm 3.3\%$) in other pyramidal cells as shown in Fig. 4*B*. The range of $EC_{50}$s estimated from fits of the data from individual cells, shown in Fig. 4*D*, *inset*, suggested three $EC_{50}$ groupings. The averaged data from all 13 cells were fitted best ($P < 0.05$) with the equation for a three-site fit (Fig. 4*D*). $EC_{50}$s estimated from the three-site model ($n_H = 1$) were 1.8, 75.8, and 275.9 nM, representing 15, 20, and 65% of the effect of diazepam to enhance 10 $\mu$M GABAR currents. Two-site fits of the diazepam data with $n_H = 2$ (Oh et al. 1995) or with a variable Hill slope, gave similar $EC_{50}$ estimates. In the former case ($n_H = 2$), a two-site fit ($EC_{50-1} = 5.6$ nM and $EC_{50-2} = 179.2$ nM) was statistically indistinguishable from a three-site fit ($EC_{50-1} = 3.3$ nM, $EC_{50-2} = 38.3$ nM, and $EC_{50-3} = 222.3$ nM).

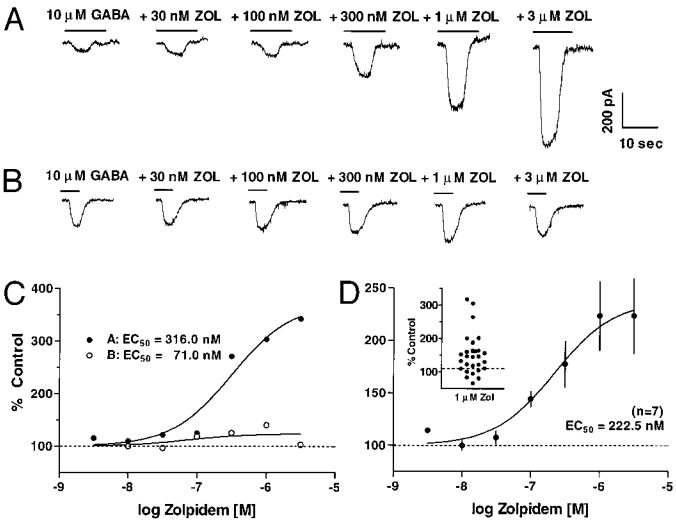


FIG. 5. Zolpidem effects on CA1 pyramidal cell GABAR currents. Zolpidem (ZOL) showed variable effects on GABAR currents. *A*: traces from an individual cell in which zolpidem enhanced GABAR currents. Not all traces are shown. Concentrations of zolpidem coapplied with 10 $\mu$M GABA are indicated *above* each trace. Bars indicate the duration of solenoid activation. *B*: traces from a different cell showing a low sensitivity to zolpidem coapplication. GABA currents in 7 of 21 cells tested with 1 $\mu$M zolpidem were insensitive to or inhibited by the imidazopyridine. *C*: concentration-response relationship for the traces in *A* and *B*. *D*: each point represents the mean (±SE) zolpidem enhancement of GABAR currents in 7 cells sensitive to zolpidem. Lines represent the best fit of the data to a sigmoidal curve. $EC_{50}$ and $n_H$ were derived from the equation for the curve. *Inset*: effect of a single concentration of zolpidem (1 $\mu$M) to potentiate GABA-induced currents in 28 CA1 pyramidal cells.

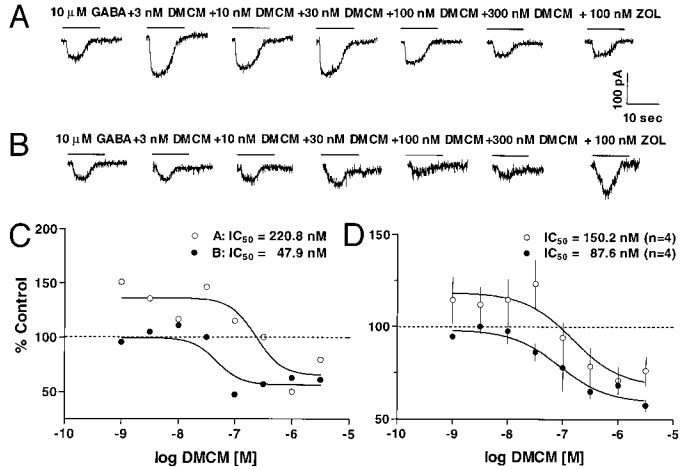


FIG. 6. Methyl 6,7-dimethoxy-4-ethyl-$\beta$-carboline-3-carboxylate (DMCM) effect on CA1 pyramidal cell GABAR currents. DMCM had biphasic effects on GABAR currents. *A*: traces are from a single cell in which DMCM enhanced GABAR currents at low concentrations. Concentrations of DMCM coapplied with 10 $\mu$M GABA are indicated *above* each trace. Not all traces are shown. Bars indicate duration of solenoid activation. *B*: traces from a different cell inhibited by DMCM coapplication. Effect of zolpidem on GABAR currents in each cell also is shown. *C*: concentration-response relationships for the traces in *A* and *B*. *D*: each point represents the mean (±SEM) DMCM effect in 4 cells in which GABAR currents were enhanced to ≥110% of control at some DMCM concentration and in 4 cells in which GABAR currents were inhibited by DMCM. Lines in *C* and *D* represent the best fit of the data to a sigmoidal curve. $IC_{50}$ and $n_H$ for each line were derived from the equations for the curves.

### *Zolpidem effects on CA1 pyramidal cell GABAR currents*

The imidazopyridine, zolpidem had variable effects on GABAR currents recorded from acutely dissociated CA1 pyramidal cells (Fig. 5). Zolpidem (1–3,000 nM) produced concentration-dependent enhancement of GABAR currents in seven of nine pyramidal cells (Fig. 5, *C* and *D*). Maximal GABAR current enhancement in these seven cells was either modest (141.9 ± 9.5%, $n = 4$) or large (308.1 ± 23.3%, $n = 3$) and could be distinguished statistically ($P < 0.02$, *t*-test with Welch's correction). The $EC_{50}$ estimated from the best-fit line (Fig. 5*D*) to the averaged data for the seven cells ($EC_{50} = 3.8–470.8$ nM) in which zolpidem enhanced GABAR currents was 222.5 nM (95% CI: 23.0–468.1 nM). In three of the nine cells (33%), GABAR currents were inhibited slightly by low concentrations of zolpidem (10–100 nM, $n = 2$) (Fig. 5, *B* and *D*) or were unchanged by zolpidem (1–1,000 nM, $n = 1$). The insensitivity to zolpidem or the inhibition of GABAR currents by zolpidem were explored further in 19 additional cells by coapplying 1 $\mu$M zolpidem with 10 $\mu$M GABA. In 8 of the 19 additional cells (42% of cells), 1 $\mu$M zolpidem inhibited (65–95% of control, $n = 6$, 32% of cells) or did not significantly enhance (110% of control, $n = 2$, 11% of cells) GABAR currents. In the remaining cells (58%), zolpidem enhancement of GABAR currents ranged from 118.0 to -201.6% (mean 153.9 ± 6.9). The responses of all cells ($n = 28$) to 1 $\mu$M zolpidem are shown in Fig. 5*D*, *inset*.

### *DMCM effects on CA1 pyramidal cell GABAR currents*

The $\beta$-carboline DMCM had variable effects on GABAR currents recorded from acutely dissociated CA1 pyramidal cells (Fig. 6). DMCM was applied with 10 $\mu$M GABA onto

eight cells. DMCM inhibited GABAR currents in half of the cells (Fig. 6, *B–D*) and had a biphasic effect on the remainder of the cells (Fig. 6, *A*, *C*, and *D*). Traces from two representative cells are shown in Fig. 6, *A* and *B*. The current traces in Fig. 6*A* show concentration-dependent enhancement of GABAR currents at low nanomolar DMCM concentrations and concentration-dependent inhibition of GABAR currents at higher concentrations. In the second cell, isolated from the same hippocampus, DMCM inhibited GABAR currents at concentrations >100 nM (Fig. 5, *B* and *C*). A few cells also were tested with 100 nM zolpidem. In the cell shown in Fig. 6*A*, the 10 $\mu$M GABA current enhanced by 3 nM DMCM was less sensitive to zolpidem than the cell in which GABA currents were only inhibited by DMCM (Fig. 6*B*). The data from individual cells were fitted best to a sigmoidal curve, and the $IC_{50}$s and $n_H$s were derived from the best-fit line. Cells in which GABAR current was enhanced by DMCM (to >110% of control) were grouped and were compared with cells in which DMCM coapplication resulted in GABAR current inhibition. Comparisons of the mean log $IC_{50}$s indicated a significant difference (Student's *t*-test, $P = 0.04$) between groups ($IC_{50} = 53.3 \pm 31.6$ nM vs. $268 \pm 103.7$ nM). The pooled data from each group are shown in Fig. 6*D*. The mean $IC_{50}$s derived from the averaged data were 87.7 nM (95% CI: 27.3–281.4 nM) and 150.2 nM (95% CI 20.5 nM to 1.1 $\mu$M), respectively.

### *Loreclezole enhancement of CA1 pyramidal cell GABAR currents*

Loreclezole had variable effects on GABAR currents recorded from acutely dissociated CA1 pyramidal cells (Fig. 7). Potentiation of GABAR currents (10 $\mu$M GABA) by loreclezole (3 nM to 10 $\mu$M) was evaluated in four cells. The maximal GABAR current enhancement produced by 10 $\mu$M loreclezole was 110–120% of the control currents (data not shown). Therefore, loreclezole (30 nM to 50 $\mu$M) was coapplied with 5 $\mu$M GABA to an additional eight pyramidal cells. Further increases in the loreclezole concentration applied were limited by its insolubility. Loreclezole concentration-dependently potentiated GABAR currents in these cells at concentrations >1 $\mu$M. A representative pyramidal cell GABAR current that was potentiated to 180% of control with 50 $\mu$M loreclezole is shown in Fig. 7, *A* and *C*. A representative pyramidal cell GABAR current that was relatively insensitive to loreclezole, i.e., potentiated to 130% of control with 50 $\mu$M loreclezole, is shown in Fig. 7, *B* and *C*. At higher concentrations (>10 $\mu$M), loreclezole produced an increase in the rate of apparent desensitization (Fig. 7, *A* and *B*) (Donnelly and Macdonald 1996). Individual loreclezole concentration-response curves were obtained for all cells (Fig. 7*C*). The $EC_{50}$s derived from individual fits ranged from 2.9 to 30.6 $\mu$M. In seven of eight cells, GABAR currents were potentiated to 155–215% of control, similar to the peak potentiation (185%) derived from the best-fit curve to the pooled data (Fig. 7*D*). The mean $EC_{50}$ estimated from the best-fit line of the averaged responses ($n = 7$) to loreclezole was 8.6 $\mu$M (95% CI: 4.9–15.1 $\mu$M).

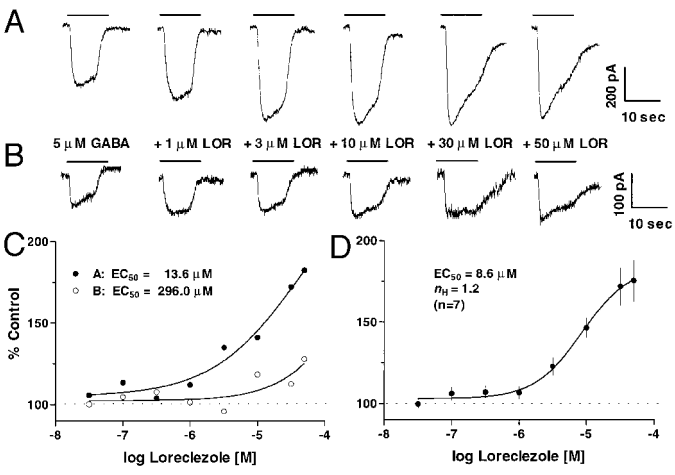


FIG. 7. Loreclezole potentiation of CA1 pyramidal cell GABAR currents. Loreclezole (LOR) enhanced GABAR currents in the majority of cells. *A*: traces were from a single cell in which loreclezole potentiated GABAR currents. Not all traces are shown. Concentrations of loreclezole coapplied with 5 $\mu$M GABA are indicated *above* each trace. Bars indicate the duration of solenoid activation. *B*: traces from a different cell showing a low sensitivity to loreclezole coapplication. *C*: concentration-response relationships for the traces in *A* and *B*. *D*: each point represents the mean (±SE) loreclezole enhancement of GABAR currents for 7 cells sensitive to loreclezole. Lines represent the best fit of the data to a sigmoidal curve. $EC_{50}$ and $n_H$ were derived from the equations for the curves.

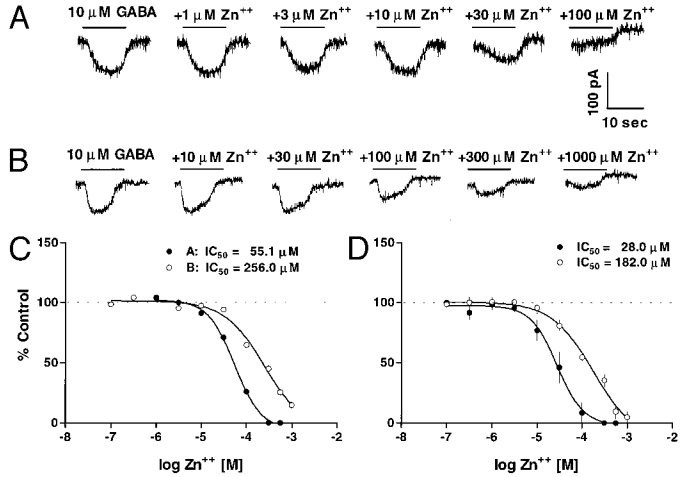


FIG. 8. Zinc inhibition of CA1 pyramidal cell GABAR currents. GABAR currents were differentially sensitive to zinc inhibition. *A*: traces from a single cell completely inhibited by 100 $\mu$M zinc. Not all currents are shown. Concentration of zinc coapplied with 10 $\mu$M GABA is indicated *above* each trace. Bars indicate the duration of solenoid activation. *B*: traces from a different cell in which GABA currents were inhibited by 50% after 100 $\mu$M zinc coapplication. *C*: concentration-response relationships for the traces shown in *A* and *B*. *D*: each point represents the mean (± SE) zinc effect on GABAR currents in 3 cells inhibited to 10% of control by 100 $\mu$M zinc and 5 cells inhibited to 50% of control by 100 $\mu$M zinc. Lines in *C* and *D* represent the best fit of the data to a sigmoidal curve. $IC_{50}$ and $n_H$ were derived from the equations for the curves.

### *Zinc inhibition of CA1 pyramidal cell GABAR currents*

Zinc had variable effects on GABAR currents recorded from acutely dissociated CA1 pyramidal cells (Fig. 8). Zinc (100 nM to 1 mM) was coapplied with GABA (10 $\mu$M) to eight pyramidal cells and reduced GABAR currents in all cells in a concentration-dependent fashion. On the basis of sensitivity to 100 $\mu$M zinc (Smart et al. 1991), data from individual cells were pooled into two groups. In five of eight cells, zinc reduced GABAR currents by ~50% ($IC_{50} = 125–978$ $\mu$M), whereas in three of eight cells, zinc reduced GABAR currents to <10% of control ($IC_{50} = 18–54$ $\mu$M, Fig. 8*C*). Representative current

traces from two cells exposed to zinc are shown in Fig. 8, *A* and *B.* In cells with a lower sensitivity to zinc, nearly complete inhibition of GABAR currents was achieved only with 1 mM zinc. A comparison of the log $IC_{50}$s estimated from individual concentration-response curves for each cell indicated a significant difference (Student's *t*-test, $P = 0.04$) between the mean log $IC_{50}$s of the two groups of cells ($IC_{50} = 32.5 \pm 10.9$ $\mu$M vs. $377 \pm 156.9$ $\mu$M). The sigmoidal fit of the concentration-response curve for the pooled data are shown in Fig. 8*D*. The $IC_{50}$s estimated from the averaged data were 28.0 $\mu$M (95% CI: 20.8–37.9 $\mu$M, $n = 3$) and 182 $\mu$M (95% CI: 74.4–447 $\mu$M, $n = 5$).

## DISCUSSION

### *GABAR currents in acutely dissociated CA1 pyramidal cells*

GABA concentration-dependently evoked inward currents on morphologically identified CA1 pyramidal cells that reversed at the predicted $E_{Cl^-}$ (Fig. 1). The voltage dependency of the GABA-induced currents in dissociated CA1 cells, i.e., outward rectification of the *I-V* relationship, was characteristic of hippocampal pyramidal cells (Ashwood et al. 1987; Burgard et al. 1996; Gray and Johnston 1985; Segal and Barker 1984). The insensitivity of pyramidal cells to baclofen indicated that GABA-induced currents were not $GABA_B$ receptor mediated. Similarly, Lenz et al. (1997) reported an absence of G-protein-mediated conductances using a high internal $[Cl^-]$ to record whole cell currents from CA1 pyramidal cells in hippocampal slices. Moreover, because inward currents in dissociated cells were blocked by bicuculline and potentiated by diazepam, it was unlikely that a component of GABA-activated currents in dissociated pyramidal cells were $GABA_C$ receptor-mediated (Bormann and Feigenspan 1995).

### *Heterogeneity of GABAR currents*

The actions of GABA on dissociated CA1 pyramidal cells suggested a functional heterogeneity of GABARs within individual cells and among different cells that was likely dependent on a variable subunit subtype composition of different GABAR isoforms. Molecular heterogeneity of GABARs was reflected in high and low affinities for GABA in receptor binding studies (c.f. Sieghart 1995). In the present study, two functionally different populations of acutely dissociated hippocampal CA1 pyramidal cells were identified based on their monophasic and biphasic GABA concentration responses, suggesting at least two affinity states of GABARs in a majority of CA1 pyramidal cells. Both populations of cells had an apparent high-affinity site for GABA similar to that reported for trypsinized CA1 pyramidal cells (6.4–14.5 $\mu$M) (Celentano and Wong 1994; Shirasaki et al. 1991). One population of dissociated cells had an apparent lower-affinity GABA site. A somewhat narrower range of GABA responses was reported for dorsal root ganglion cells isolated from adult rats (26–107 $\mu$M) (White 1992), consistent with the diversity of GABAR subunit mRNAs in those cells (Persohn et al. 1991). The range of GABA $EC_{50}$s in dissociated CA1 cells was within the range of $EC_{50}$s for recombinant GABARs assembled in oocytes and embryonic kidney 293 cells from various subunit combinations (1.3–42 $\mu$M, Levitan et al. 1988; 9–985 $\mu$M, Sigel et al. 1990; 17–103 $\mu$M, Verdoorn et al. 1990) and may reflect the 15-fold difference in sensitivity of at least two $\beta$-subunit polypeptides ($M_r$ 55,000 and 58,000) to $GABA_A$ agonists (Bureau and Olsen 1990).

The range of $EC_{50}$s associated with the GABAR high-affinity state in dissociated cells also could represent more than one high-affinity site. For example, two cultured hippocampal cell populations, differentiated according to their GABA-induced desensitization rates, both had high affinities for GABA (8.5 and 37.3 $\mu$M) (Schönrock and Borrmann 1993), similar to the range of high-affinity $EC_{50}$s detected in dissociated cells. Conversely, discrepancies between GABAR potencies in cell culture and young adult rat brain are not unexpected. Expression of GABAR subunit mRNAs is regulated developmentally in the CA1 region (Gambarana et al. 1991; Möhler et al. 1995), coincident with the late appearance of $\gamma$-aminobutyric acid decarboxylase (GAD) immunoreactive cells (Potier et al. 1992) and of functional GABAergic inhibition in the CA1 region (Harris and Teyler 1983; Michelson and Lothman 1992).

Overall, the data suggested that the two GABAR affinity states detected may reflect that at least two functionally distinct populations of GABARs were localized to different regions of the pyramidal cell and/or that different GABAR isoforms existed among distinct populations of pyramidal cells. These data are consistent with earlier reports of pharmacologically and electrophysiologically distinguishable GABAR responses in CA1 pyramidal cell somata and dendrites (Alger and Nicoll 1982). More recently, two anatomically and functionally distinct GABAR-mediated synaptic responses, i.e., $GABA_{A,\ fast}$ and $GABA_{A,\ slow}$, were detected using both intracellular and whole cell recordings in CA1 pyramidal cells in in vitro hippocampal slices (Banks et al. 1998; Pearce 1993). On the basis of immunocytochemical colocalization of the $\alpha$2 and $\beta$1 subtypes, the former on the axon initial segment (Benke et al. 1994; Chen et al. 1996; Möhler et al. 1995; Nusser et al. 1996; E. I. Tietz, S. Chen, and W. Sieghart, unpublished observations), $\alpha2\beta1\gamma2$ receptors are likely prominent CA1 pyramidal cell GABAR isoforms, perhaps mediating the $GABA_{A,fast}$ response (Pearce 1993). The colocalization of $\alpha$1 and $\beta$3 subtypes on pyramidal cell processes (Chen et al. 1996; Nusser et al. 1996; Sperk et al. 1997; E. I. Tietz, S. Chen, and W. Sieghart, unpublished observation) suggests that GABARs composed of $\alpha1\beta3\gamma2$ subtypes could represent the second class of functionally and anatomically distinct GABARs, perhaps mediating the dendritic $GABA_{A,slow}$ response proposed to underlie the classical, early inhibitory postsynaptic potential (Banks et al. 1998; Pearce 1993). The immunostaining pattern of other subtype antibodies would allow a role for the $\alpha$5, but not $\alpha$3, subtype in mediating either of the proposed $GABA_{A,fast}$ or $GABA_{A,slow}$ responses (Fritschy and Möhler 1995).

### *Cell-to-cell heterogeneity*

In contrast to the biphasic GABA responses in CA1 pyramidal cells, GABA concentration-response curves obtained in young adult dentate granule cells, many isolated from the same hippocampi used in the present study, were all monophasic ($EC_{50} = 47$ $\mu$M) (Kapur and Macdonald 1996). Because pyramidal cells and granule cells display a different complement of GABAR subtype mRNAs (Wisden et al. 1992) and pattern of GABAR subtype protein immunostaining (Fritschy and Möhler 1995; Nusser et al. 1996; Somogyi et al. 1996;

Sperk et al. 1997; E. I. Tietz, S. Chen, and W. Sieghart, unpublished observations), these contrasting findings strengthen the likelihood that the unique pharmacological actions of GABA on hippocampal principal cell types was dependent on GABAR subunit subtype composition.

The contrasting responses of hippocampal CA1 pyramidal cells, dentate granule cells, and other neuron populations to GABA and allosteric modulators supports the hypothesis that GABAR isoform heterogeneity is one basis for the diversity of GABA inhibitory function within the hippocampus and other neuronal circuits (Banks et al. 1998; Kapur and Macdonald 1996; Möhler et al. 1995; Pearce 1993). Nevertheless, post-translational modifications or other factors, e.g., phosphorylation state of the receptor, also might contribute to the different GABAR-mediated current pharmacology among hippocampal neuronal subtypes (Geynes et al. 1994; Leidenheimer et al. 1991; Macdonald and Olsen 1994; Smart 1997; Stelzer 1992). This possibility could not be distinguished in the present study. Moreover, heterogeneity of GABAR isoforms also probably is related to differences in chloride channel properties, e.g., rectification and desensitization, ascribed to hippocampal neuronal populations (Birnir et al. 1994; Burgard et al. 1996; Gray and Johnston 1985; Pearce 1993; Schönrock and Bormann 1993).

### *Heterogeneity of allosteric regulation of GABAR currents*

Added variation in the functional response of GABARs in pyramidal cells was only evident in the presence of allosteric modulators, entirely consistent with classical binding studies that identified two GABA binding sites and a diverse allosteric modulator pharmacology (c.f. Doble and Martin 1992; Sieghart 1995). Allosteric modulators that interact with the benzodiazepine binding site on GABARs, i.e., diazepam, zolpidem, and DMCM, produced multiphasic modulation of GABAR currents consistent with a mixed Type I/Type II benzodiazepine pharmacology (Doble and Martin 1992). The modulation of CA1 pyramidal cell GABAR currents by allosteric modulators disclosed a large degree of GABAR heterogeneity that was not always readily predicted from the GABAR subtype mRNA and protein expressed in CA1 pyramidal cells (Fritschy and Möhler 1995; Nusser et al. 1996; Somogyi et al. 1996; Sperk et al. 1997; Wisden et al. 1992; E. I. Tietz, S. Chen, and W. Sieghart, unpublished observations).

The responses to diazepam were consistent with the existence of multiple GABAR isoforms containing low- and mid- or low- and high-affinity benzodiazepine binding sites. Multiple nanomolar $EC_{50}$s also were reported for clonazepam potentiation of GABAR currents in thalamic and cortical neurons dissociated from early postnatal, juvenile and young adult rats (Oh et al. 1995). Alternately, potentiation of dentate granule cell GABAR currents by diazepam was reported to be monophasic ($EC_{50}$ = 158 nM) (Kapur and Macdonald 1996). The distribution and relative abundance of $\alpha$ subunit subtype mRNAs ($\alpha5 > \alpha2 \gg \alpha1 = \alpha4 \ggg \alpha3$) in CA1 pyramidal cells (Williamson and Pritchett 1994; Wisden et al. 1992) and the pattern of $\alpha$ subtype immunostaining in the CA1 region (c.f. Fritschy and Möhler 1995) suggest that native GABARs composed of $\alpha1$, $\alpha2$, and/or $\alpha5$ subtypes most likely contributed to the heterogeneity of the diazepam responses in CA1 pyramidal cells. The overall benzodiazepine sensitivity of CA1 cells also was expected to relate to their $\gamma2$ subtype mRNA and protein expression, although a contribution of $\gamma1$ subtype-containing native GABARs to the multiphasic effects of diazepam to enhance GABAR currents could not be excluded (Knoflach et al. 1991; Somogyi et al. 1996; Wisden et al. 1992). Pyramidal cell GABARs also might contain multiple $\alpha$ (McKernan et al. 1991; Verdoorn 1994) or $\beta$ subtypes (Li and De Blas 1997). Studies of the structural domains of the benzodiazepine binding sites reinforce the primary importance of variations in $\alpha$ and $\gamma$ GABAR subunit subtype composition in determining benzodiazepine pharmacology (Smith and Olsen 1995). Nonetheless, diazepam potentiation of GABAR currents in oocytes was shown to vary 4- to 12-fold with $\beta$ subtype substitution (Sigel et al. 1990), suggesting that the quaternary structure of native GABARs also may affect benzodiazepine pharmacology.

The monophasic zolpidem concentration-response function was consistent with the presence of primarily moderate affinity, BZ Type IIA receptors, although a small population of higher-affinity BZ Type I receptors might be represented by the lower percentage of cells with the lowest $EC_{50}$, consistent with the absence of $\alpha1$ subtypes on the soma proximal dendrites of ~35% of pyramidal cells (Nusser et al. 1996). The remaining cells were insensitive to or inhibited by 1 $\mu$M zolpidem, consistent with the presence of BZ Type IIB (or BZ Type III) receptors with negligible zolpidem affinity (Lüddens et al. 1994; McKernan et al. 1991; Pritchett et al. 1989). Zolpidem-insensitive CA1 pyramidal cells exhibited more rectification and less desensitization at depolarized potentials than zolpidem-sensitive cells, similar to properties described in recombinant $\alpha5\beta1\gamma2$L and $\alpha5\beta3\gamma2$L GABARs expressed on mouse L929 fibroblasts (Burgard et al. 1996). Combined with the results of binding studies using recombinant GABARs (Lüddens et al. 1994) and in situ hybridization studies (Wisden et al. 1992), these findings suggested that an $\alpha5\beta3\gamma2$L GABAR isoform was also likely to be expressed on CA1 pyramidal cells. The pattern of zolpidem sensitivity/insensitivity may reflect the presence of $\alpha1$, $\alpha2$, and $\alpha5$ subtype mRNAs and protein (Fritschy and Möhler 1995; Nusser et al. 1996; Williamson and Pritchett 1994; Wisden et al. 1992) consistent with the detection of three binding sites ($K_D$ = 15 nM, 225 nM and 6 $\mu$M) for [$^3$H]zolpidem in the hippocampus (Ruano et al. 1992) and a triphasic diazepam concentration response.

DMCM both enhanced and inhibited GABAR currents in dissociated pyramidal cells. The positive modulatory effect of DMCM at low concentrations in 50% of the cells tested suggested the presence of either the $\alpha5$ or $\gamma1$ subtypes, shown in recombinant GABARs to confer positive modulatory actions on DMCM (Puia et al. 1991; von Blankenfeld et al. 1990). The relatively low expression of the $\gamma1$ subtype, in comparison with the $\alpha5$ subtype, mRNA (Fritschy and Möhler 1995; Wisden et al. 1992), suggested that potentiation of GABAR currents by DMCM may more likely be due to the functional assembly of $\alpha5\beta x\gamma2$ GABARs, consistent with their reduced sensitivity to zolpidem. The monophasic inhibitory response of hippocampal dentate granule cells to DMCM ($EC_{50}$ = 60 nM) (Kapur and Macdonald 1996) also might be explained by the relatively lower levels of $\alpha5$ subtype mRNA and protein expression compared with CA1 pyramidal cells (Fritschy and Möhler 1995; Wisden et al. 1992). The relative contribution of $\alpha1$ or $\alpha2$ subtype-containing GABARs to the inhibitory effects of DMCM on GABAR currents (Puia et al. 1991; von Blankenfeld et al. 1990) could not be deduced from the data.

Loreclezole enhanced GABAR currents in the majority of cells with an $EC_{50}$ similar to that reported in dentate granule cells (9 $\mu$M), although a larger fraction (50%) of granule cells were loreclezole insensitive (Kapur and Macdonald 1996). These findings were consistent with the relatively lower levels of expression of $\beta$1 subtype mRNAs and protein in granule cells than in CA1 pyramidal cell somata (Wisden et al. 1992; E. I. Tietz, S. Chen and W. Sieghart, unpublished observations).

Two distinct populations of CA1 pyramidal cells were separated by the extent of inhibition produced by zinc. The relative insensitivity of some CA1 pyramidal cells to 100 $\mu$M zinc, a concentration previously used to establish zinc insensitivity of $\gamma$2 subtype-containing GABAR isoforms (Smart et al. 1991), was consistent with the presence of the $\gamma$2 subtype (Fritschy and Möhler 1995; E. I. Tietz, S. Chen and W. Sieghart, unpublished observations) and the sensitivity of dissociated cells to benzodiazepine agonists. Nevertheless, this could not explain the moderate zinc sensitivity of the remaining fraction of pyramidal cells tested. Dentate granule cells also showed a uniformly moderate zinc sensitivity ($IC_{50}$ = 29 $\mu$M) (Kapur and Macdonald 1996). Consistent with the ability of $\alpha$ subtypes to modulate zinc sensitivity (Fisher and Macdonald 1997; Saxena and Macdonald 1996), GABAR currents in mouse fibroblasts containing $\alpha5\beta3\gamma2$L subtypes were moderately zinc sensitive ($IC_{50}$ = 22 $\mu$M) (Burgard et al. 1996). This finding raises the possibility that zolpidem-insensitive GABAR isoforms in CA1 pyramidal cells may have contributed to the appearance of two populations of cells with different zinc sensitivities.

### *Comparison of heterogeneity of allosteric regulation and GABAR subtype expression*

On the basis of allosteric modulator responses in dissociated cells and responses obtained in recombinant receptors expressing known subunit subtype combinations, certain functional GABAR subtype combinations were likely to be predominant on CA1 pyramidal cells. Although classical benzodiazepine agonists have relatively equivalent binding affinities among $\alpha$1, $\alpha$2, or $\alpha$5 subtype-containing recombinant receptors (cf. Doble and Martin 1992), their relative potencies at functional pentameric receptors assembled in heterologous systems varied more widely (Sigel et al. 1990), consistent with the range of action of diazepam in dissociated CA1 pyramidal cells as indicated by the three diazepam affinity states detected. The lack of $\alpha$1 subtype immunoreactivity on a fraction of pyramidal cell somata, the localization of the $\alpha$2 subtype on the axon initial segment (Nusser et al. 1996), coupled with the high levels of $\alpha$5 mRNA and protein expression on CA1 pyramidal cells (Fritschy and Möhler 1995; Wisden et al. 1992), would suggest a predominance of Type IIA ($\alpha$2 subtype-containing) and Type IIB ($\alpha$5 subtype-containing) benzodiazepine receptors on CA1 pyramidal cell GABARs (Doble and Martin 1992). Although less prominent, the existence of functional BZ Type I ($\alpha$1 subtype) receptors cannot be ruled out based on the presence of $\alpha$1 subtype-immunopositive synapses on a subpopulation of CA1 pyramidal cell somata and on their processes (Nusser et al. 1996; Zimprich et al. 1991) and the increased sensitivity of a small fraction of dissociated cells to zolpidem.

The predominance of BZ Type IIB ($\alpha$5 subtype-containing) receptors was consistent with the responses to all of the allosteric modulators tested. Given the insensitivity of some CA1 pyramidal cell GABAR currents to zolpidem, the positive modulatory actions of DMCM in some cells and their loreclezole sensitivity, an $\alpha5\beta3\gamma2$ GABAR isoform was likely present on $\geq$30% of individual pyramidal cells. The enhancement of GABAR currents by diazepam in all cells studied implies that a large fraction of GABAR isoforms contained the $\gamma$2 subtype (Fritschy and Möhler 1995, Sperk et al. 1997; Wisden et al. 1992; E. I. Tietz, S. Chen and W. Sieghart, unpublished). Nevertheless, the sensitivity of some cells to zinc supports the possibility that a portion of native pyramidal cell GABAR isoforms coexpress the $\alpha$5 subtype as found with $\alpha5\beta3\gamma2$ recombinant receptors (Burgard et al. 1996).

Taken together, the findings of the present study suggest that the subtype-specific expression of GABARs can provide an additional method for modulating the functional properties of individual hippocampal pyramidal cells, consistent with the hypothesis that the diversity of GABA actions in the CNS are related to the assembly of multiple GABAR isoforms on individual neurons, among populations of neurons and within specific functional neuronal pathways or brain regions (Burt and Kamatchi 1991; Möhler et al. 1995; Nusser et al. 1996) and reinforcing the likelihood that GABAR heterogeneity plays an important role in regulating GABAR inhibition within the hippocampal trisynaptic circuit.

We thank Dr. Andrew Beavis for assistance with the derivation of model equations and N. Esmaeil for technical assistance.

This work was supported by National Institutes of Health Grants K02-DA-00180 (E. I. Tietz), K08-NS-01748 (J. Kapur), and R01-NS-33300 (R. L. Macdonald).

Address for reprint requests: E. I. Tietz, Dept. of Pharmacology, Medical College of Ohio, Block Health Science Bldg., 3035 Arlington Ave., Toledo, OH 43614-5804.

Received 1 December 1997; accepted in final form 17 December 1998.

## REFERENCES

ALGER, B. E. AND NICOLL, R. A. Pharmacological evidence for two kinds of GABA receptors on rat hippocampal pyramidal cells studied in vitro. *J. Physiol. (Lond.)* 328: 125–141, 1982.

ASHWOOD, T. J., COLLINGRIDGE, G. L., HERRON, C. E., AND WHEAL, H. V. Voltage-clamp analysis of somatic $\gamma$-aminobutyric acid responses in adult rat hippocampal CA1 neurones in vitro. *J. Physiol. (Lond.)* 384: 27–37, 1987.

BANKS, M. I., LI, T.-B., AND PEARCE, R. A. The synaptic basis of $GABA_{A,slow}$. *J. Neurosci.* 18: 1305–1317, 1998.

BENKE, D., FRITSCHY, J.-M., TRZECIAK, A., BANNWARTH, W., AND MÖHLER, H. Distribution, prevalence, and drug binding profile of $GABA_A$ receptor subtypes differing in $\beta$ subunit isoform. *J. Biol. Chem.* 269: 27100–27107, 1994.

BIRNIR, B., EVERITT, A. B., AND GAGE, P. W. Characteristics of $GABA_A$ channels in rat dentate gyrus. *J. Membr. Biol.* 142: 93–102, 1994.

BORMANN, J. AND FEIGENSPAN, A. $GABA_C$ receptors. *Trends Neurosci.* 18: 515–519, 1995.

BORMANN, J., HAMILL, O. P., AND SAKMANN, B. Mechanism of anion permeation through channels gated by glycine and $\gamma$-aminobutyric acid in mouse cultured spinal neurones. *J. Physiol. (Lond.)* 385: 243–286, 1987.

BROOKS-KAYAL, A. R., JIN, H., PRICE, M., AND DICHTER, M. A. Developmental expression of GABA(A) receptor subunit mRNAs in individual hippocampal neurons in vitro and in vivo. *J. Neurochem.* 10: 1017–1028, 1998.

BUREAU, M. AND OLSEN, R. W. Multiple distinct subunits of the $\gamma$-aminobutyric acid-A receptor protein show different ligand binding affinities. *Mol. Pharmacol.* 37: 497–502, 1990.

BURGARD, E. C., TIETZ, E. I., NEELANDS, T. R., AND MACDONALD, R. L. Properties of recombinant γ- aminobutyric $acid_A$ receptor isoforms containing the α5 subunit subtype. *Mol. Pharmacol.* 50: 119–127, 1996.

BURT, D. R. AND KAMATCHI, G. L. $GABA_A$ receptor subtypes: from pharmacology to molecular biology. *FASEB J.* 5: 2916–2923, 1991.

CELENTANO, J. J., GYENES, M., GIBBS, T. T., AND FARB, D. H. Negative modulation of the γ-aminobutyric acid response by extracellular zinc. *Mol. Pharmacol.* 40: 766–773, 1991.

CELENTANO, J. J. AND WONG, R.K.S. Multiphasic desensitization of the $GABA_A$ receptor in outside-out patches. *Biophys. J.* 66: 1039–1050, 1994.

CHEN, S., HUANG, X., ZENG, X. J., AND SIEGHART, W. Benzodiazepine-mediated regulation of α1-2, β1-3 and γ2 $GABA_A$ receptor subunit proteins in the rat brain hippocampus and cortex. *Neuroscience*. In press.

DAVIES, P. A., HANNA, M. C., HALES, T. G., AND KIRKNESS, E. Insensitivity to anaesthetic agents conferred by a class of $GABA_A$ receptor subunit. *Nature* 385: 820–823, 1997.

DOBLE, A. AND MARTIN, I. L. Multiple benzodiazepine receptors: no reason for anxiety. *Trends Pharmacol. Sci.* 13: 76–81, 1992.

DONNELLY, J. AND MACDONALD, R. L. Loreclezole inhibition of recombinant $GABA_A$ receptor isoforms expressed in L929 fibroblasts. *Neuropharmacology* 35: 1233–1241, 1996.

DRAGUHN, A., VERDORN, T. A., EWERT, M., SEEBURG, P. H., AND SAKMANN, B. Functional and molecular distinction between recombinant rat $GABA_A$ receptor subtypes by $Zn^{2+}$. *Neuron* 5: 781–788, 1990.

DUCIC, I., CARUNCHO, H. J., ZHU, W. J., VICINI, S., AND COSTA, E. γ-Aminobutyric acid gating of $Cl^-$ channels in recombinant $GABA_A$ receptors. *J. Pharmacol. Exp. Ther.* 272: 434–445, 1995.

DUTAR, P. AND NICOLL, R. A. A physiological role for $GABA_B$ receptors in the central nervous system. *Nature* 332: 156–158, 1988.

EBERT, B., WAFFORD, K. A., WHITING, P. J., KROGSGAARD-LARSEN, P., AND KEMP, J. A. Molecular pharmacology of γ-aminobutyric acid type-A receptor agonists and partial agonists in oocytes injected with different α, β and γ receptor subunit combinations. *J. Pharmacol. Exp. Ther.* 46: 957–963, 1994.

EHLERT, F. J., ROESKE, W. R., GEE, K. W., AND YAMAMURA, H. I. An allosteric model for benzodiazepine receptor function. *Biochem. Pharmacol.* 32: 2375–2383, 1993.

FISHER, J. L. AND MACDONALD, R. L. The role of α1 and α6 subtype amino-terminal domains in allosteric regulation of γ-aminobutyric $acid_A$ receptors. *Mol. Pharmacol.* 52: 714–724, 1997.

FREUND, T. F. AND BUZSÁKI, G. Interneurons of the hippocampus. *Hippocampus* 6: 347–470, 1996.

FRITSCHY, J.-M., BENKE, D., MERTENS, S., OERTEL, W. H., BACHI, T., AND MOHLER, H. Five subtypes of type A GABA receptors identified in neurons by double and triple immunofluorescence staining with subunit-specific antibodies. *Proc. Natl. Acad. Sci. USA* 89: 6726–6730, 1992.

FRITSCHY, J.-M. AND MOHLER, H. $GABA_A$-receptor heterogeneity in the adult rat brain: differential regional and cellular distribution in seven major subunits. *J. Comp. Neurol.* 359: 154–194, 1995.

GAMBARANA, C., BEATTIE, C. E., RODRIGUEZ, Z. R., AND SIEGEL, R. E. Region-specific expression of messenger RNAs encoding $GABA_A$ receptor subunits in the developing rat brain. *Neuroscience* 45: 423–432, 1991.

GEYNES, M., WANG, Q., GIBBS, T. T., AND FARB, D. H. Phosphorylation factors control neurotransmitter and neuromodulator actions at the γ-aminobutyric acid type A receptor. *Mol. Pharmacol.* 34: 542–549, 1994.

GRAY, R. AND JOHNSTON, D. Rectification of single GABA-gated chloride channels in adult hippocampal neurones. *J. Neurophysiol.* 54: 134–142, 1985.

GREENFIELD, L. J., JR. AND MACDONALD, R. L. Whole-cell and single-channel α1β1γ2S $GABA_A$ receptor currents elicited by a ''multipuffer'' drug application device. *Pflügers Arch. Eur. J. Physiol.* 432: 1080–1090, 1996.

HADINGHAM, K. L., WINGROVE, P. B., WAFFORD, K. A., BAIN, C., KEMP, J. A., PALMER, K. J., WILSON, A. W., WILCOX, A. S., SIKELA, J. M., RAGAN, C. I., AND WHITING, P. J. Role of the β subunit in determining the pharmacology of human γ-aminobutyric acid type A receptors. *Mol. Pharmacol.* 44: 1211–1218, 1993.

HAMILL, O. P., MARTY, A., NEHER, E., SAKMANN, B., AND SIGWORTH, F. J. Improved patch-clamp techniques for high-resolution current recording from cells and cell-free membrane patches. *Pflügers Arch.* 391: 85–100, 1981.

HARRIS, K. M. AND TEYLER, T. J. Evidence for late development of inhibition in area CA1 of the rat hippocampus. *Brain Res.* 268: 339–343, 1983.

KAPUR, J. AND MACDONALD, R. L. Pharmacological properties of $GABA_A$ receptors from acutley dissociated rat dentate granule cells. *Mol. Pharmacol.* 50: 458–466, 1996.

KAY, A. R. AND WONG, R. K. Isolation of neurons suitable for patch-clamping from adult mammalian central nervous systems. *J. Neurosci. Methods* 16: 227–238, 1986.

KNOFLACH, F., RHYNER, T., VILLA, M., KELLENBERGER, S., DRESCHER, U., MALHERBE P., SIGEL, E., AND MÖHLER, H. The $\gamma_3$-subunit of the $GABA_A$-receptor confers sensitivity to benzodiazepine receptor ligands. *FEBS Lett.* 293: 191–194, 1991.

LACAILLE, J.-C., KUNKEL, D. D., AND SCHWARTZKROIN, P. A. Electrophysiological and morphological characterization of hippocampal interneurons. In: *The Hippocampus—New Vistas.* New York: Alan R. Liss, 1989, p. 287–305.

LEIDENHEIMER, N. J., BROWNING, M. D., AND HARRIS, R. A. $GABA_A$ receptor phosphorylation: multiple sites, actions and artifacts. *Trends Pharmacol. Sci.* 12: 84–87, 1991.

LENZ, R. A., PITLER, T. A., AND ALGER, B. E. High intracellular $Cl^-$ concentrations depress G-protein-modulated ionic conductances. *J. Neurosci.* 17: 6133–6141, 1997.

LEVITAN, E. S., BLAIR, L.A.C., DIONNE, V. E., AND BARNARD, E. A. Biophysical and pharmacological properties of cloned GABA receptor subunits expressed in *xenopus* oocytes. *Neuron* 1: 773–781, 1988.

LI, M. AND DE BLAS, A. L. Coexistence of two β subunit isoforms in the same γ-aminobutyric acid Type A receptor. *J. Biol. Chem.* 272: 16564–16569, 1997.

LÜDDENS, H., SEEBURG, P. H., AND KORPI, E. R. Impact of β and γ variants on ligand-binding properties of γ-aminobutyric acid Type A receptors. *Mol. Pharmacol.* 45: 810–814, 1994.

MACDONALD, R. L. AND ANGELOTTI, T. P. Native and recombinant $GABA_A$ receptor channels. *Cell Physiol. Biochem.* 3: 352–373, 1993.

MACDONALD, R. L. AND OLSEN, R. W. $GABA_A$ receptor channels. *Annu. Rev. Neurosci.* 17: 569–602, 1994.

MCKERNAN, R. M., QUIRK, K. L., PRINCE, R., COX, P. A., GILLARD, N. P., RAGAN, C. I., AND WHITING, P. $GABA_A$ receptor subtypes immunopurified from rat brain with α subunit specific antibodies have unique pharmacological properties. *Neuron* 7: 667–676, 1991.

MCKERNAN, R. M., WAFFORD, K., QUIRK, K. L., HADINGHAM, E. A., HARLEY, C. I., AND WHITING, P. I. The pharmacology of the benzodiazepine site of the GABA-A receptor is dependent on the type of γ subunit present. *J. Recept. Signal Transduction Res.* 15: 173–183, 1995.

MICHELSON, H. B. AND LOTHMAN, E. W. Ontogeny of epileptogenesis in the rat hippocampus: a study of the influence of GABAergic inhibition. *Brain Res. Dev. Brain Res.* 66: 237–243, 1992.

MILES, R., TOTH, K., GULYAS, A. I., HAJOS, N., AND FREUND, T. F. Differences between somatic and dendritic inhibition in the hippocampus. *Neuron* 16: 515–523, 1996.

MÖHLER, H., KNOFLACH, F., PAYSAN, J., MOTEJLEK, K., BENKE, D., LÖSCHER, B., AND FRITSCHY, J.-M. Heterogeneity of $GABA_A$-receptors: cell specific expression, pharmacology, and regulation. *Neurochem. Res.* 20: 631–636, 1995.

NAYEEM, H., GREEN, T. P., MARTIN, L. L., AND BARNARD, E. A. Quaternary structure of the native $GABA_A$ receptor determined by electron microscopic image analysis. *J. Neurochem.* 62: 815–818, 1994.

NEWBERRY, N. B. AND NICOLL, R. A. Comparison of the action of baclofen with γ-amminobutyric acid on rat hippocampal pyramidal cells in vitro. *J. Physiol. (Lond.)* 360: 161–185, 1985.

NUSSER, Z., SIEGHART, W., BENKE, D., FRITSCHY, J. M., AND SOMOGYI, P. Differential synaptic localization of two major gamma-aminobutyric acid type A receptor alpha subunits on hippocampal pyramidal cells. *Proc. Natl. Acad. Sci. USA* 93: 11939–11944, 1996.

OH, K.-S., LEE, C.-J., GIBBS, J. W., AND COULTER, D. A. Postnatal development of $GABA_A$ receptor function in somatosensory thalamus and cortex: whole-cell voltage-clamp recordings in acutely isolated rat neurons. *J. Neurosci.* 15: 1341–1351, 1995.

OLSEN, R. W., MCCABE, R. T., AND WAMSLEY, J. K. $GABA_A$ receptor subtypes: autoradiographic comparison of GABA, benzodiazepine, and convulsant binding sites in rat central nervous system. *J. Chem. Neuroanat.* 3: 59–76, 1990.

PEARCE, R. A. Physiological evidence for two distinct $GABA_A$ responses in rat hippocampus. *Neuron* 10: 189–200, 1993.

PERSOHN, P., MAHLERBE, P., AND RICHARDS, J. G. In situ hybridization histochemistry reveals a diversity of $GABA_A$ receptor subunit mRNAs in neurons of the rat spinal cord and dorsal root ganglia. *Neuroscience* 42: 497–507, 1991.

POTIER, B., RASCOL, O., JAZAT, F., LAMOUR, Y., AND DUTAR, P. Alterations in the properties of hippocampal pyramidal neurons in the aged rat. *Neuroscience* 48: 793–806, 1992.

PRITCHETT, D. B., SONTHEIMER, H., SHIVERS, B. D., YMER, S., KETTENMANN, H., SCHOFIELD, P. R., AND SEEBURG, P. H. Importance of a novel GABA(A) receptor subunit for benzodiazepine pharmacology. *Nature* 338: 582–585, 1989.

PUIA, G., VICINI, S., SEEBURG, P. H., AND COSTA, E. Influence of recombinant $\gamma$-aminobutyric acid$_A$ receptor subunit composition on the action of allosteric modulators of $\gamma$-aminobutyric acid-gated $Cl^-$ currents. *Mol. Pharmacol.* 39: 691–696, 1991.

RUANO, D., VIZUETE, M., CANO, J., MACHADO, A., AND VITORICA, J. Heterogeneity in the allosteric interaction between the $\gamma$-aminobutyric acid (GABA) binding site and three different benzodiazepine binding sites of the GABA$_A$/benzodiazepine receptor complex in the rat nervous. *J. Neurochem.* 58: 485–491, 1992.

SAXENA, N. C. AND MACDONALD, R. L. Assembly of GABA$_A$ receptor subunits: role of the delta subunit. *J. Neurosci.* 14: 7077–7086, 1994.

SAXENA, N. C. AND MACDONALD, R. L. Properties of putative cerebellar $\gamma$-aminobutyric acid$_A$ receptor isoforms. *Mol. Pharmacol.* 49: 567–579, 1996.

SEGAL, M. AND BARKER, J. L. Rat hippocampal neurons in culture: properties of GABA-activated $Cl^-$ ion conductance. *J. Neurophysiol.* 51: 500–515, 1984.

SCHÖNROCK, B. AND BORMANN, J. Functional heterogeneity of hippocampal GABA$_A$ receptors. *Eur. J. Neurosci.* 5: 1042–1049, 1993.

SHIRASAKI, T., KLEE, M. R., NAKAYE, T., AND AKAIKE, N. Differential blockade of bicuculline and strychnine on GABA-and glycine-induced responses in dissociated rat hippocampal pyramidal cells. *Brain Res.* 561: 77–83, 1991.

SIEGHART, W. Structure and pharmacology of $\gamma$-aminobutyric acid$_A$ receptor subtypes. *Pharmacol. Rev.* 47: 181–234, 1995.

SIGEL, E., BAUR, R., TRUBE, G., MÖHLER, H., AND MAHLERBE, P. The effect of subunit composition of rat brain GABA$_A$ receptors on channel function. *Neuron* 5: 703–711, 1990.

SMART, T. G. Regulation of excitatory and inhibitory neurotransmitter-gated ion channels by protein phosphorylation. *Curr. Opin. Neurobiol.* 7: 367–368, 1997.

SMART, T. G., MOSS, S. J., XIE, X., AND HUGANIR, R. L. GABA$_A$ receptors are differentially sensitive to zinc: Dependence on subunit composition. *Br. J. Pharmacol.* 103: 1837–1839, 1991.

SMITH, G. B. AND OLSEN, R. W. Functional domains of GABA$_A$ receptors. *Trends Pharmacol. Sci.* 16: 167–168, 1995.

SOMOGYI, P., FRITSCHY, J.-M., BENKE, D., ROBERTS, J.D.B., AND SIEGHART, W. The $\gamma$2 subunit of the GABA receptor is concentrated in synaptic junctions containing the $\alpha$1 and $\beta$2/3 subunits in hippocampus, cerebellum and globus pallidus. *Neuropharmacology* 35: 1425–1444, 1996.

SPERK, G., SCHWARZER, C., TSUNASHIMA, K., FUCHS, K., AND SIEGHART, W. GABA$_A$ receptor subunits in the rat hippocampus I: immunocytochemical distribution of 13 subunits. *Neuroscience* 80: 987–1000, 1997.

STALEY, K., OTIS, T. S., AND MODY, I. Membrane properties of dentate gyrus granule cells: comparison of sharp microelectrode and whole cell recordings. *J. Neurophysiol.* 57: 1346–1358, 1992.

STELZER, A. Intracellular regulation of GABA$_A$-receptor function. In: *Ion Channels.* New York: Plenum, 1992, p. 83–136.

STELZER, A., KAY, A. R., AND WONG, R.K.S. GABA(A)-receptor function in hippocampal cells is maintained by phosphorylation factors. *Science* 241: 339–341, 1988.

VERDOORN, T. A. Formation of heteromeric $\gamma$-aminobutyric acid type A receptors containing two different subunits. *Mol. Pharmacol. Ther.* 45: 475–480, 1994.

VERDOORN, T. A., DRAGUHN, A., YMER, S., SEEBURG, P. H., AND SAKMANN, B. Functional properties of recombinant rat GABA$_A$ receptors depend upon subunit composition. *Neuron* 4: 919–928, 1990.

VINCINI, S. Pharmacological significance of the structural heterogeneity of the GABA$_A$ receptor-chloride ion channel complex. *Neuropsychopharmacology* 4: 9–15, 1991.

VON BLANKENFELD, G., YMER, S., PRITCHETT, D. B., SONTHEIMER, H., EWERT, M., SEEBURG, P. H., AND KETTENMANN, H. Differential benzodiazepine pharmacology of mammalian recombinant GABA$_A$ receptors. *Neurosci. Lett.* 115: 269–273, 1990.

WAFFORD, K. A., BAIN, C. J., QUIRK, K., MCKERNAN, R. M., WINGROVE, P. B., WHITING, P. J., AND KEMP, J. A. A novel allosteric modulatory site on the GABA$_A$ receptor $\beta$ subunit. *Neuron* 12: 775–782, 1994.

WHITE, G. Heterogeneity of $EC_{50}$ and $n_H$ of GABA$_A$ receptors on dorsal root ganglion neurons freshly isolated from adult rats. *Brain Res.* 585: 56–62, 1992.

WIELAND, H. A., LÜDDENS, H., AND SEEBURG, P. H. A single histidine in GABA$_A$ receptors is essential for benzodiazepine agonist binding. *J. Biol. Chem.* 267: 1426–1429, 1992.

WILLIAMSON, R. E. AND PRITCHETT, D. B. Levels of benzodiazepine receptor subtypes and GABA$_A$ receptor $\alpha$-subunit mRNA do not correlate during development. *J. Neurochem.* 63: 413–418, 1994.

WISDEN, W., LAURIE, D. J., MONYER, H., AND SEEBURG, P. H. The distribution of 13 GABA$_A$ receptor subunit mRNAs in the rat brain. I. Telencephalon, diencephalon, mesencephalon. *J. Neurosci.* 12: 1040–1062, 1992.

ZIMPRICH, F., ZEZULA, J., SIEGHART, W., AND LASSMANN, H. Immunohistochemical localization of the $\alpha$1, $\alpha$2 and $\alpha$3 subunit of the GABA$_A$ receptor in the rat brain. *Neurosci. Lett.* 127: 125–128, 1991.